Climate Dynamics
https://doi.org/10.1007/s00382-022-06217-0

Regional earth system modelling framework for CORDEX-SA: an integrated model assessment for Indian summer monsoon rainfall

Pankaj Kumar[1] · Alok Kumar Mishra[1] · Aditya Kumar Dubey[1] · Aaquib Javed[1] · Md. Saquib Saharwardi[1] · Amita Kumari[1] · Disha Sachan[1] · William Cabos[2] · Daniela Jacob[3] · Dmitry V. Sein[4,5]

Received: 12 October 2021 / Accepted: 15 February 2022
© The Author(s), under exclusive licence to Springer-Verlag GmbH Germany, part of Springer Nature 2022

Abstract
An effort is made to implement a regional earth system model (RESM); ROM, over CORDEX-South Asia (SA). The added value of RESM is assessed for mean precipitation, its variability (intraseasonal to interannual), extremes, and associated processes. In this regard, ROM's fields are compared with the respective fields of its standalone version (REMO), the models belonging coupled model intercomparison project (CMIP5 and CMIP6), and regional climate models of CORDEX-CORE simulations. RESM shows substantial improvement for most of the Indian monsoon's aspects; however, the magnitude of the value addition varies spatiotemporally and also with different aspects.. The improved representation of intraseasonal variability (active-break spell's duration and intensity) and Interannual variability attributed to improved mean seasonal precipitation. Additionally, correct representation of sea surface temperature, Indian Ocean Dipole, and its underlying dynamics also contribute to improving the mean precipitation. The notable improvement is seen especially over the south-eastern regions of the Bay of Bengal (BoB) and South-Central India, where increasing (decreasing) low-pressure systems over Central India (BoB) are noticed as a consequence of air-sea coupling, leading to enhanced (reduced) precipitation over Central India (BoB), reducing dry (wet) bias found in REMO and the other models. Despite substantial improvements, RESM has a systematic wet bias in the mean precipitation associated with a warm bias over the western coast of the Arabian Sea. An overestimation of very high extreme precipitation due to the enhanced contribution of low-pressure systems indicates the model's limitations, suggesting the need for further tuning of the RESM.

1 Introduction

The Indian summer monsoon is one of the strongest monsoon systems in the world, contributing 80% of the annual precipitation over India (Gadgil et al. 1984). It impacts the agriculture and life of more than one billion people, thus controlling the economy of the country (Gadgil and Gadgil 2006). However, the complex physical mechanisms and interactions with the highly complex South-Asian physiography always make it a great challenge for climate modelers to accurately simulate the Indian summer monsoon rainfall (ISMR) (Turner and Annamalai 2012). Coupled atmosphere–ocean general circulation models (AOGCM) or earth system models (ESMs) are the most sophisticated tools available to investigate global climate and its driving mechanisms e.g., models that participated in the coupled model intercomparison project (CMIP) are widely used for climate change studies of all parts of the globe, including the Indian monsoon. Despite great efforts to develop the most advanced version—CMIP6 (Stockhause and Lautenschlager 2017), with improved physics and refinements of resolution with respect to their previous versions [CMIP5; Taylor et al. (2012) and CMIP3; Meehl et al. (2007)]—they are still unable to resolve local and regional forcing, especially in a complex region like the Indian subcontinent. Moreover, a strong inter-model spread in the simulated fields of these

✉ Pankaj Kumar
kumarp@iiserb.ac.in

1 Department of Earth and Environmental Sciences, Indian Institute of Science Education and Research, Bhopal 462066, India

2 Departmento de Física y Matemáticas, Universidad de Alcalá, Madrid, Spain

3 Climate Service Center Germany (GERICS), Helmholtz-Zentrum Hereon, Hamburg, Germany

4 Alfred Wegener Institute for Polar and Marine Research, Bremerhaven, Germany

5 Shirshov Institute of Oceanology, Russian Academy of Science, Moscow, Russia

Published online: 03 March 2022

models, especially in the tropics (Li et al. 2018; Wu et al. 2019), limits the confidence in the model to project climate signals. The coarser horizontal and absence of regional (fine-scale) air-sea interaction restricting the use of GCMs or ESMs for many aspects of monsoon(Fu et al. 2007), particularly extremes and propagation of low-pressure systems (LPSs) (Stowasser et al. 2009; Levine et al. 2020), northward propagation of the boreal summer intraseasonal oscillation (BSISO) (Sabeerali et al. 2013; Li et al. 2018), and active-break spells (Sharmila et al. 2015; Misra et al. 2018).

The uncertainties in these models raise questions on the reliability of projections on a regional scale climate (Sperber et al. 2013; Saha et al. 2014), demanding to improve the understanding and advances in the numerical and physical formulations of climate models, especially the high-resolution regional climate models (RCMs) (Giorgi et al. 2009). The downscaling of the output of GCMs or ESMs using RCMs provides a finer-scale detail relative to the parent model that added value in simulating the Indian summer monsoon precipitation regional scale. Although numerous studies attempted to assess the RCM's skill over the coordinated regional downscaling experiments for South Asia (CORDEX-SA) region, a clear overview of the overall performance of RCM experiments remains unclear. Some studies show improvement in reproducing the spatial distribution and precipitation intensity (Lucas-Picher et al. 2011; Saha et al. 2011; Kumar et al. 2013, 2014; Dash et al. 2014, 2015; Parth Sarthi et al. 2015; Pattnayak et al. 2018; Mishra et al. 2020a, b; Maharana et al. 2021; Mishra and Dubey 2021). However, RCMs still show a substantial bias, particularly dry bias over Central India (CI). The missing ocean dynamics or regional air-sea interaction and feedback processes in RCMs limit the predictability of the tightly coupled processes like the Indian summer monsoon (ISM) (Ratnam et al. 2009; Xue et al. 2020; Mishra et al. 2021a, b). This emphasized the necessity of a regional atmosphere–ocean coupled model (RAOCM) or regional earth system model (RESM) for accurately representing the interactions amongst different components of the climate system during the ISM, particularly at spatial scales that are not resolved by global models (Ratnam et al. 2009; Giorgi and Gao 2018; Giorgi 2019).

Numerous regional atmosphere–ocean coupled models or RESMs have been developed during recent decades that include multiple components, such as atmosphere, oceans, sea ice, hydrology, land, and marine biogeochemistry, and used widely for a broad range of applications, including the study of climate change simulations across different parts of the world (Drobinski et al. 2012; Sein et al. 2014, 2015, 2020; Wang et al. 2015b; Giorgi and Gutowski 2016; Sitz et al. 2017). Earlier, attempts were made to develop a fully coupled high-resolution regional model having varying components of earth systems and its complexities for the different parts of the globe (Hagedorn et al. 2000; Sitz et al. 2017; Sevault et al. 2014; Ruti et al. 2016; Reale et al. 2020). Sevault et al. 2014 investigated the performance of a fully coupled model for Mediterranean regional and showed good performance. Ruti et al. (2016) reported the advantage of RESM for MED-CORDEX. Reale et al. 2020 investigated the performance of a fully coupled regional earth system model in which, RegCM is taken as an atmospheric component, and MITgcm is taken as an ocean component and reported substantial improvement for Mediterranean climate and marine biogeochemistry. Most of the studies noticed a significant improvement in both ocean and atmospheric fields due to air-sea coupling. Comparatively, lesser efforts have been made to develop RESM for the Indian monsoon (Samala et al. 2013; Di Sante et al. 2019; Mishra et al. 2021a, b) and investigate the various aspects of ISM. These studies reported substantial improvement in simulating ISMR, however, it still shows notable dry bias over central India (Mishra et al. 2020a, 2021a), considerably larger than the ROM model used in this study. Most of the studies for LPSs and their contribution to ISMR (Levine et al. 2020) reported significant improvements due to air-sea coupling.

In this study, we have implemented a state-of-the-art high-resolution RESM, namely ROM, over CORDEX-SA. The previously discussed RESMs have only selectively focused on few aspects, the moderate horizontal resolution (~ 50 km), and for a shorter integration period. Giorgi and Gutowski (2016) indicated that a horizontal resolution of 20–30 km is essential to sufficiently represent the topographic effects on climate change. Thus, this study rigorously accesses the performance of the RESM for a long simulation period (38 years) and adequately high resolution (~ 25 km) for many of the ISM aspects, including LPS, that act as a major contributor (~ 60%) of rainfall over the Indian subcontinent (Krishnamurthy and Ajayamohan 2010; Sandeep et al. 2018) and variability of various time scales (intraseasonal to interannual). This model has been previously tested over the Atlantic and Pacific sector and has shown better skills than the standalone RCM simulations for most of the climate variables such as circulation, temperature, and precipitation (Sein et al. 2014). This study aims to contribute to the CORDEX South Asia framework initiative with a first detailed assessment of high-resolution RESM simulations. The evaluation of the ROM output becomes even more relevant in the sense that this model has not been explored over CORDEX-SA (Mishra et al. 2021b). This study will help in understanding the relative benefit.

2 Model and methodology

2.1 Models description

The regional Earth system model, ROM, used in this study, comprises of the atmosphere, ocean, land, sea ice, and biogeochemical and hydrological components that are interactively coupled to each other. In this coupled system, the regional atmosphere model (REMO; Jacob 2001) is used as an atmospheric component, which is coupled with the soil model (Rechid et al. 2009). The Max Planck Institute Ocean Model (MPIOM; Marsland et al. 2002) coupled with the Hamburg Ocean Carbon Cycle (HAMOCC) model (Maier-reimer et al. 2005) and dynamic-thermodynamic sea ice model (Hibler 1979) is adopted as the oceanic component. The Hydrological Discharge model (HD; Hagemann and Dümenil 1998) is used for the terrestrial hydrology simulation that exchanges the fields with atmosphere and ocean. The OASIS coupler (Valcke 2013) ensures coupling between the different components with a coupling frequency of three hours of model time for the atmosphere and the ocean and one day for the HD model. We took three hours of coupling frequency as it is necessary to resolve the diurnal cycle. All models are run in a global configuration except REMO, which is coupled over CORDEX-SA. The domain is adequately large to develop its large-scale monsoonal circulation and the cross-equatorial flow. The atmosphere–ocean coupling is implemented over CORDEX-SA, which is systematically represented in Fig. 1. The REMO delivers heat fluxes, freshwater flux, wind stress, and surface air pressure to MPIOM, whereas the MPIOM exchanges sea surface temperature (SST), sea ice thickness and concentration (if present) to REMO.

i. Atmospheric components

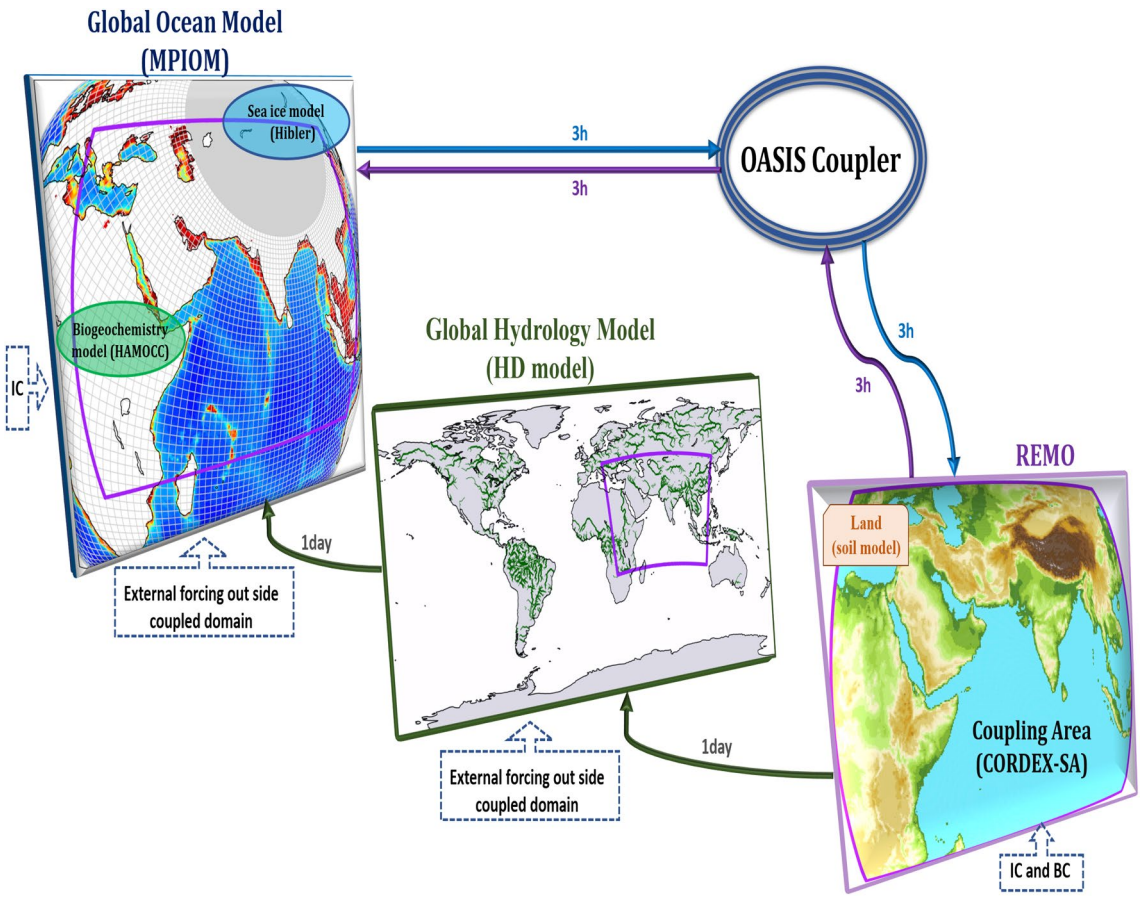

Fig. 1 Systematic representation of the Regional Earth System Model (RESM) over the CORDEX-South-Asia region. The rectangle box in every panel shows the RESM coupling region. Arrows represent the interaction among different components. The left panel shows the bathymetry of the global ocean model, and the contour shows its variable resolution grid (drawn every 5th line). The middle panel shows the drainage network (green lines) for the global HD model. The right panel shows regional model (REMO) topography in meters. The coupling between REMO and MPIOM is done using the OASIS coupler. The coupling frequency is 3-hourly. The IC and BC indicate the Indian and boundary conditions

REMO is a hydrostatic, three-dimensional regional climate atmospheric model whose physical parameterizations are adopted from the global climate model ECHAM versions 4 and 5 (Roeckner et al. 2003). The leap-frog scheme with time filtering by Asselin (1972) is used for temporal discretization and the Arakawa-C-grid, for spatial discretization. REMO employed the rotated geographical coordinates system in horizontal and hybrid vertical coordinates. The rotated grid warrants the disproportion issues of grids closer to the poles. We use 0.22 (~ 25 km) horizontal resolution and 27 hybrid vertical levels. The six-hourly varying fields obtained from ECMWF ERA-Interim (T255 gaussian grid, i.e. ca. 75 km horizontal resolution) (Dee et al. 2011) are used for lateral boundary conditions that are relaxed in the outer eight grids of the model following the method of (Davies 1976). This sponge zone is excluded from the analysis. The fractional land surface scheme is adopted for the land-surface process (Rechid et al. 2009). The physics and spectral dynamics such as cumulus convection, mixing, heat and momentum transfer, and horizontal and vertical diffusion in REMO are adopted from ECHAM (Roeckner et al. 2003). A mass flux scheme for cumulus convection (Tiedtke, 1989) and a statistical cloud cover scheme of Tompkins (2002), and heat and momentum, flux is formulated using the analytical expressions of Louis (1979).

The model results are stored for 38 years from 1 January 1980 to 31 December 2017 after removing the initial transients (100 years of stand-alone ocean spinup and following 50 years of coupled model spinup). For the simulation of ISM during the present climate, long-term simulations are carried out using ROM and its standalone atmospheric component REMO, with the same model set up over the CORDEX-SA domain. We adopted the common configuration and model domain (CORDEX-SA) for standalone and coupled simulation. The SST obtained from ECMWF ERA-Interim is prescribed as external forcing in the standalone run, while MPIOM supplied SST to REMO in the coupled run. The atmospheric fields obtained from the ERAI reanalysis are used as initial and boundary conditions for the standalone and coupled run.

ii. Oceanic components

The MPIOM (Jungclaus et al. 2013) is taken as the oceanic component of the ROM and contains the sea ice model (Hibler 1979) and ocean biogeochemistry using a HAMburg Ocean Carbon Cycle model (HAMOCC, Maier-Reimer et al. 2005). The MPIOM is customized globally, differentiating it from most of the earlier regional earth system models (which generally use regionally configured ocean models) adopted over South Asia. Global customization takes care of the several issues created by inconsistencies between the regional model solution and lateral boundary data (provided by the global ocean reanalysis/ model). For example,reducing the uncertainty arising from the lateral boundary conditions, as the prescription of lateral boundary conditions in regional ocean models is one of the key problems and sources of damping error from the global ocean reanalysis/model datasets through a boundary on timescales of less than a month (Sein et al. 2015, 2020; Parras-Berrocal et al. 2020).

MPIOM has an orthogonal curvilinear grid facility that facilitates varying horizontal resolution. This adopts a maximum resolution of 5 km (eddy-permitting) over the coastal region, ~ 10–20 km in the Indian Ocean (IO), and a minimum resolution of about 100 km in the Tropical Atlantic. The ocean is divided vertically into 40 unevenly spaced levels following a z-level coordinate. We employed bottom boundary layer slope convection (Marsland et al. 2003). The mixing scheme of PP (Pacanowski and Philander) (Pacanowski and Philander, 1981, JPO) is adopted in MPIOM. The atmospheric fields (heat flux, freshwater flux, wind stress, and surface air pressure) obtained from the ECMWF ERA-Interim (ERAI) reanalysis (Dee et al. 2011) are prescribed as external atmospheric forcing outside the coupled domain, while REMO supplies these forcings over the coupled domain. The model is also equipped with tidal forcing (Thomas et al. 2001), generally absent in most global ESM.

iii. Hydrological components

ROM employed a Hydrological Discharge model (HD) (Hagemann and Du¨menildu¨menil 1998), which is integrated globally with 0.5° horizontal resolution. HD as a subroutine of REMO gets runoff and drainage from REMO (over the coupled region), reads runoff and drainage obtained from reanalysis (globally), combines them, and calculates global river runoff into the ocean. After all the calculations, HD writes river runoff into the file (once per day), and MPIOM reads this file.

2.2 Experiment design and data used

We have used different observation and reanalysis data sets to assess the model performances. ERA5 [ERA5; Buchwitz et al. 2018] reanalysis data of '850-hPa winds at three-hourly intervals and 31 km horizontal resolution are used for diagnosing monsoon LPS and monthly mean ERA5 data for atmospheric winds. ERA5 is the latest updated version of

the very popular ERA Interim reanalysis, which is based on the advanced Integrated Forecasting System (IFS) with improved model physics, core dynamics, and data assimilation. Various studies have highlighted the importance of the ERA5 (Hersbach et al. 2020), and the ERA5-based modeling performance is reported to be equivalent to observation datasets (Mahto and Mishra 2019).

The high spatial (10 km) and temporal (3-hourly) resolution Multi-Source Weighted Ensemble Precipitation (MSWEP) data is used to assess the ROM's performance in simulating the precipitation. This data consists of precipitation estimates from satellite (infrared and microwave), rain gauge, and reanalysis (Beck et al. 2019). The study by Beck et al. (2019), evaluated 22 precipitation products, and the MSWEP product is reported to be one of the best performers. We also compared the MSWEP with India Meteorological Department (IMD) and ERA5 for 1998–2016 (common period of the availability of all source's data) period (Fig. S1), which indicated a good resemblance between precipitation. The Hadley Centre Global Sea Ice and Sea Surface Temperature (HadISST) data (Rayner et al. 2003) evaluates ROM's simulated SST. Three-hourly wind obtained from ERA5 is used to compute the vorticity for tracking the LPS. Similarly, three-hourly accumulated total precipitation is used to estimate the precipitation associated with LPS.

To investigate the added value of ROM over GCMs and RCMs, we employed the precipitation of CMIP5/6 models and RCMs of CORDEX-SA simulation with the same forcing of ERAI. The details for CMIP5/6 and CORDEX-SA RCMs are given in Table S1&S2.

2.3 LPS tracking methodology

(a) Tracking algorithm

A tracking algorithm has been applied to the 3-hourly lower-tropospheric vorticity field for the 38 JJAS seasons (1980–2017) of the two regional models: REMO and ROM, and the reanalysis dataset ERA5 to understand the impact of precipitation associated with LPS in the core monsoon region. The tracking algorithm, called "TRACK," has been extensively used in various tracking studies worldwide (Rastogi et al. 2018; Curio et al. 2019; Hoskins and Hodges 2019). The LPS tracking for each dataset is done at 850 hPa (Sandeep et al. 2018). The vertically averaged vorticity is then spatially filtered using spherical harmonics to T63 resolution, with the large-scale background also removed. Vorticity maxima are determined on the T63 grid and then used as starting points to obtain the off grid locations using B Spline interpolation and maximization methods (Hodges 1995). All positive vorticity centers that exceed a threshold value of $1.0 \times 10–5\ s^{-1}$ are joined together to produce a coherent set of tracks for their full life cycles (Hodges 1999; Pinheiro et al. 2020; Lakkis et al. 2021). This is performed by initializing a set of tracks based on the nearest neighbor method and then refined by minimizing a cost function for track smoothness, subject to adaptive constraints for displacement and track smoothness (Hodges 1995, 1999). After the tracking, the full-resolution precipitation is associated with each point of the tracks to infer their impact. In this study, precipitation is averaged over an area within an 8° radius around each LPS track point (Hunt et al. 2018; Hunt and Fletcher 2019).

(b) Filtering algorithm

IMD provides a challenging definition of LPS (also called monsoon lows and depressions) to work with. It states that "The monsoon lows and depressions are the principal rain-bearing systems of the southwest monsoon period over India. Substantial amounts of rainfall are generated by the westward passage of monsoon depressions forming in the Bay of Bengal. These are low-pressure areas having wind speeds between 17 and 33 knots in their circulation. The Maximum wind strength and intensity can be noticed at the levels of 0.9 km or 1.5 km (~ 850 hPa). These can be of Bay origin, Land origin or Arabian Sea origin" (IMD 2015). The tracks were then made to undergo three-level filtering criteria, which are defined below:

i. Firstly, only those tracks that sustained themselves for at least three days and traveled a minimum distance of 1000 km for the regional models (500Kms for ERA5) are considered for the study. The difference in traveling distance arises from the fact that LPSs were observed to travel more in regional models when compared to the reanalysis dataset.
ii. To infer the impact of LPS over the core monsoon zone, the filtered tracks obtained at level-1 then go through the second round of filtering, which involves identifying those tracks which pass through our region of interest. A Lat-Lon box boundary (to be called "Impact Boxes" henceforth; 15°–25° N and 78°–92° E), characterizing the core monsoon region and as defined by Sandeep et al. (2018), is used to achieve the purpose.

The tracks from level-2 are then filtered based on their genesis over land and ocean.

2.4 Vertically integrated moisture ux (VIMF)

The VIMF is computed over 1000–300 hPa, following Konwar et al. (2012) using the following equation.

–

where q is specific humidity, u and v are zonal and meridional components of wind, p represents the.

pressure and g is the acceleration due to gravity.

2.5 Inter-tropical convergence zone (ITCZ)

The seasonal ITCZ migration is depicted using precipitation data for two reference datasets (MSWEP and ERAI) and REMO and ROM. The daily precipitation data for each of the four datasets are averaged over 1980–2017 and smoothed temporally and meridionally by a locally-weighted linear regression (LOESS) method, spanning four days in time and 0.25° in latitude, ultimately used to decide the position of ITCZ from the points of zonally-averaged rainfall maxima (Schneider et al. 2014). The corresponding spatial patterns of precipitation over the land and the ocean, characterizing the ITCZ migration and position during the June–September (JJAS) season, are also included in the study.

2.6 Active and break spell

The active and break spells are defined as the events with precipitation greater than + -1 standardized anomaly for at least three consecutive days during the peak monsoon months i.e. July and August, over the core monsoon regions (Rajeevan et al. 2010; Singh et al. 2014). Moreover, we categorised the active and break spells into short and long spells as well. 3–4 days persisting active events are considered as the short active spells, while events persisting for greater than 4 days are the long active events. However, the short and long break events are defined as the events persisting for 3–6 days and > 6 days, respectively (Dwivedi et al. 2015).

3 Results

In this study, we rigorously assess the skill of a new Regional Earth System Model (RESM) in simulating the various aspects of ISM characteristics, which will be briefly discussed later. Notably, this model is used for the first time to simulate the Indian summer monsoon, which would be useful as a future roadmap for Regional Earth System Modeling framework (RESMF), to address the mechanism behind climate change, including detection, attribution, and future projections over CORDEX-SA.

3.1 Demonstration of model skill for mean and variability

Figure 2a–d represents a comparison of the mean precipitation during summer monsoon season (June-July–August–September; JAJS) of the study period from the models, observation, and parent-driven reanalysis (ERAI). The corresponding bias is also shown in Fig. 2e–g. The spatial pattern of precipitation is characterized by a zone of precipitation maxima over the windward side (west coast of India, Myanmar, and foothills of Himalayas); over Bangladesh, extended up to central India; and rain shadow area (leeward side) over the east coast of India, Western Ghats (WG) as well as minimal precipitation over northwest India (NWI) and Pakistan (Kumar et al. 2014). The models show good skill in recognizing the spatially-varying precipitation maxima and minima regions; however, they show a limitation in capturing the magnitude and cause some key spatial patterns to shift, e.g., both simulations overestimate rainfall over South-Central India (SCI), compared to observations. REMO shows an unrealistic precipitation maxima region over a large area of Western Central India (WCI) (~ 15–20 mm/day) while it is in the range of 5–10 mm/day in observation. ROM indicates a clear improvement by reducing this unrealistic precipitation.

For climate models, it is always challenging to simulate orographic rainfall regimes (e.g., WG) and reduce the long persisting dry bias over the Indo-Gangetic belt (IGB) and CI. Apart from this, the overestimation of precipitation over the BoB and the south IO is a general problem of most of the RCMs (Ratnam et al. 2009; Lucas-Picher et al. 2011). Interestingly, both models show clear improvement over WG relative to ERAI. Barring a few places (WG and Indo Gangetic plains), ROM shows very little bias (1.5 mm/day), which is relatively less than the bias noticed in its atmospheric component (REMO), parents forcing (ERAI), as well as the ensemble mean of the RCMs that participated in the CORDEX simulation driven by ERAI (same forcing as in ROM) and CMIP5/6 (Fig. S2). ROM's simulated bias is relatively lesser than the earlier studies using high-resolution RESM (Misra et al. 2017; Di Sante et al. 2019; Mishra et al. 2021a, b). In general, ROM shows substantial improvement over most of the regions in terms of the spatial representation and intensity of precipitation; however, the magnitude of the added values varies spatially.

To make the results more perspective in terms of quantitative assessment, we computed statistical Taylor metrics, such as correlation coefficient (CC), ratio, root mean square error (RMSE), that are shown in the Taylor diagram for JJAS mean precipitation during 1980–2005 (the common period of available data sets for all sources). For CMIP5 and CMIP6, the ensemble of the multi-model has been considered. The detail of these data set has been given in

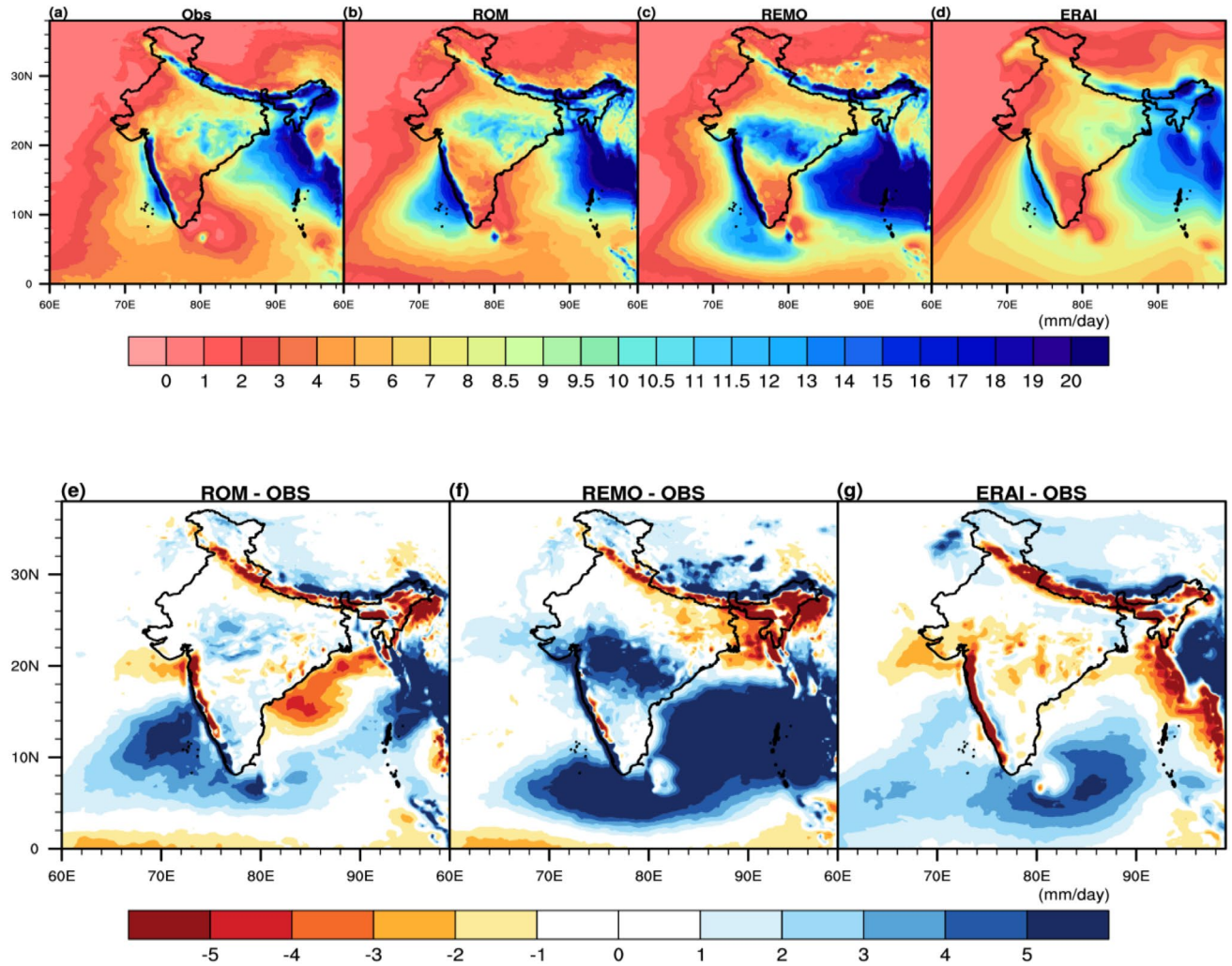

Fig. 2 Mean precipitation duringthe summer monsoon season (June–July–August; September; JAJS) of the study period from the a observation, b ROM c REMO d parent-driven reanalysis (ERAI). Corresponding bias for e ROM f REMO and g ERAI

supplementary table 1 and 2. Taylor diagram uses the whole period mean at each grid point and then after all the statistics were calculated. In this figure, the best-performing model has the highest pattern correlation and least bias and unity ratio with respect to the reference data.It is observed that ROM fences off the coupled GCMs, CORDEX RCMs, as well as their standalone REMO's skill in resembling the observation (lowest RMSE), thus confirming the advantage of high-resolution regional air-sea coupling (see Fig. 3).

The strength and sub-seasonal variation of IMSR is strongly governed by the migration (northward/southward propagation) of the ITCZ. It maintains the north–south gradient, which is tightly coupled with monsoon progression and withdrawal processes. Thus, assessing the model skill in simulating the ITCZ is worthwhile. Figure 4 shows the annual cycle of ITCZ for ROM, REMO, and observation during 1980–2017. Observation shows the mean position of ITCZ over the south of the equator from October to April. In May, it crosses the equator and shows a gradual northward movement, reaching 25° N in mid-June and stays there till mid of August. Then, it sharply migrates towards the south and crosses the equator by the end of September. In REMO, the ITCZ swings between the average latitudes of 15° N in summer and 20° S in winter, prompting the skewness toward the southern hemisphere. Apart from this, the ITCZ migrates northward unrealistically early in the last week of April and swings at its maximum northward latitude for a longer time, facilitating the favorable condition for warmup and deep convection, even after the real retreat of monsoon, indicating the early onset and late retreat of the monsoon, and hence, lengthening the rainy season (Fig. S3). ROM substantially minimizes these discrepancies that presented in its counterpart REMO, further highlighting the advantage of air-sea coupling. The continuous energy supply and

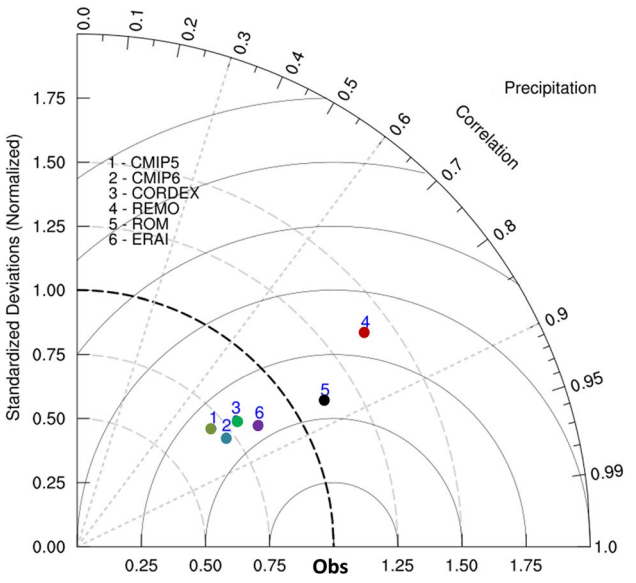

Fig. 3 Taylor diagram for ROM's evaluation. These statistics are computed for JJAS mean during 1980–2005 (common period of all data sources) for each grid point over Indian land points

moisture being pumped from the underlying prescribed SST maintain excessive convection due to the absence of negative feedback in the uncoupled model, REMO. Meanwhile, the presence of negative feedback in the coupled model, ROM, leads to lower SSTs, caused by convective cooling, which reduces the air-sea fluxes and weakens the convection. As compared to its driving forcing of ERAI, ROM shows the dual nature of change, improving the performance during the withdrawal phase and degrading during the onset phase. Despite improvements, some discrepancies still exist in the ROM during the onset and peak phase, suggesting that the inclusion of air–sea coupling alone is not enough to improve all discrepancies, thereby demanding further improvement of physics and tuning of the atmospheric model itself.

The intraseasonal variabilities (ISVs) characterized by the active and break phases of rainfall exert a critical control on mean precipitation and interannual variability (Krishnamurthy and Kinter, 2003) and are largely regulated by the air-sea interaction. Despite improving the understanding and development in the recent era, ISVs simulations by GCMs continue to depict a large bias (Sperber and Annamalai 2008; Sperber et al. 2013). In recent decades, the importance of regional coupled models has been highlighted in improving the ISVs (Misra et al. 2017; Di Sante et al. 2019; Mishra et al. 2021a). Thus, we evaluate the skills of ROM and REMO and quantify the advantage of air–sea coupling in simulating the active-break spells. The active and break spell are computed using the criteria by Rajeevan et al. (2010). We computed the number and duration of active and break spells during the study period along with their duration and frequency (Fig. S4 and Table S3) from models and corresponding observations. ROM's simulated temporal evolution of the active-break spells is closer to observation than REMO and ERAI in terms of their frequency and duration. ROM's simulated active and break spells are in the phase of corresponding observation with some systematic differences. In general, observation shows, on average, a greater (lesser) duration of active (break) spells. Both ROM and REMO are able to reproduce the asymmetrical distribution of the active-break spell duration. It is observed that the duration and frequency of the active spells are increasing. ROM shows noticeable improvements in simulating the trend; however, REMO fails to do so and even produces negative trends in contrast to observation. Relatively less skill is noticed for break spells in ROM.

A study by Dwivedi et al. (2015) showed that the differential frequency of occurrence for short/long break and active spells regulates the asymmetry in precipitation during spells of active/break. Following Dwivedi et al. (2015), active (break) spells are divided into two categories, namely, short and long spells. Break spells of three-seven days and greater than seven days are considered as short break spells (SBS) and long break spells (LBS). Similarly, active spells of three to four days and greater than four days are considered short active spells (SAS) and long active spells (LAS). Figure S5 reveals that both ROM and REMO show better performances relative to driven ERAI in terms of the duration and frequency of short and prolonged active and break spells. For short spells, ROM does not show an improvement over REMO; however, substantial improvement is noticed for prolonged spells.

The simulation of the IAV of ISMR plays an extremely crucial role in the long prediction of ISM, which is largely controlled by local and remote air-sea interaction (Krishna Kumar 2005; Zhu and Shukla 2013) and very challenging for the modeling community to simulate it. Thus, it is worthwhile to access the model's skill and quantify the advantage of air–sea coupling in representing the IAV. Figure 5 shows that the ROM reproduces interannual variability precipitation reasonably well. ROM shows relatively better performance than REMO in distinguishing the years of positive/negative precipitation anomaly in the phase of corresponding observation. The correlation coefficients between ROM (REMO) and observation are 0.32 (0.06), statistically significant at the 95% confidence level. Although this correlation (0.32) is lower, however, it is higher than the skills of earlier reported operational statistical models and global-coupled climate models (Wang et al. 2015a). A noticeable improvement is observed in ROM toward the well-documented years of extreme wet rainfall (e.g., 1883, 1994, 2007, 2013) that are not satisfactorily represented by most of the earlier models (GCMs/RESMs) (Chaudhari et al. 2013). Interestingly, ROM

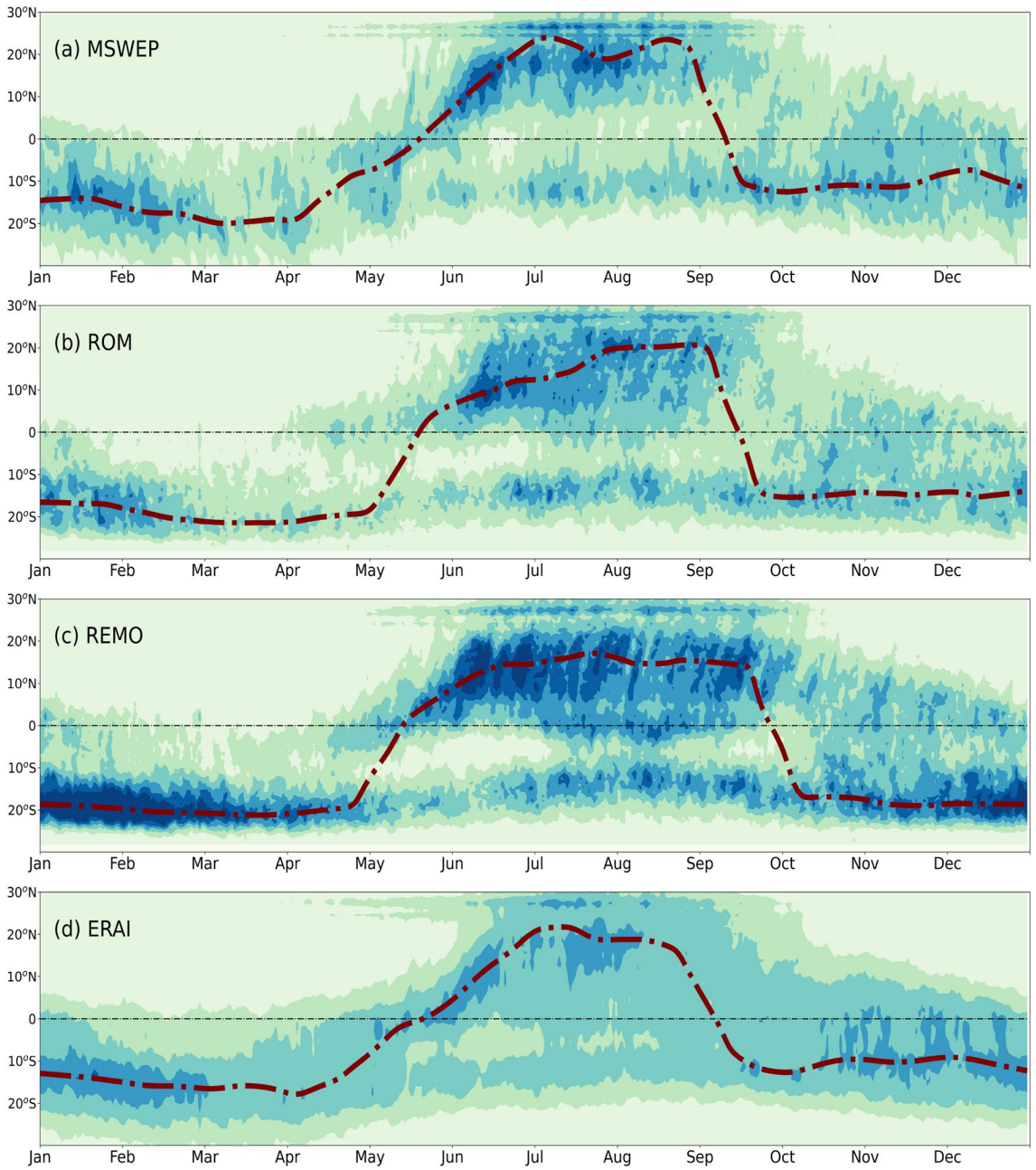

Fig. 4 Intertropical convergence zone (ITCZ) for ROM, REMO, ERAI, and Observation

correctly reproduces the sign of the anomalous wet years 1994 and 2013, which co-occurred with a stronger positive IOD. However, REMO and earlier studies (Chaudhari et al. 2013) show signs of drought during these years. A recent study by Di Sante et al. (2019) performed a high-resolution RESM over CORDEX-SA, which showed an improved IAV relative to the corresponding standalone atmospheric components; however, it was not able to reproduce the correct sign for the rainfall anomaly of 1994. This shows the clear advantage of air–sea coupling and the potential of our regional coupled model setups. ROM also shows reasonable improvement towards drought in comparison to REMO. For example, the year 1986 is depicted as a drought year in ROM in the observation phase, whereas REMO represents this year as a flood year. ROM fails to capture some drought years e.g., 1987, 2009. ROM shows a greater skill for extreme climate associated with the wet condition than dry conditions. The model's poor skill in simulating the IAV of ISMR partially arises from an improper simulation of some important phenomenon and

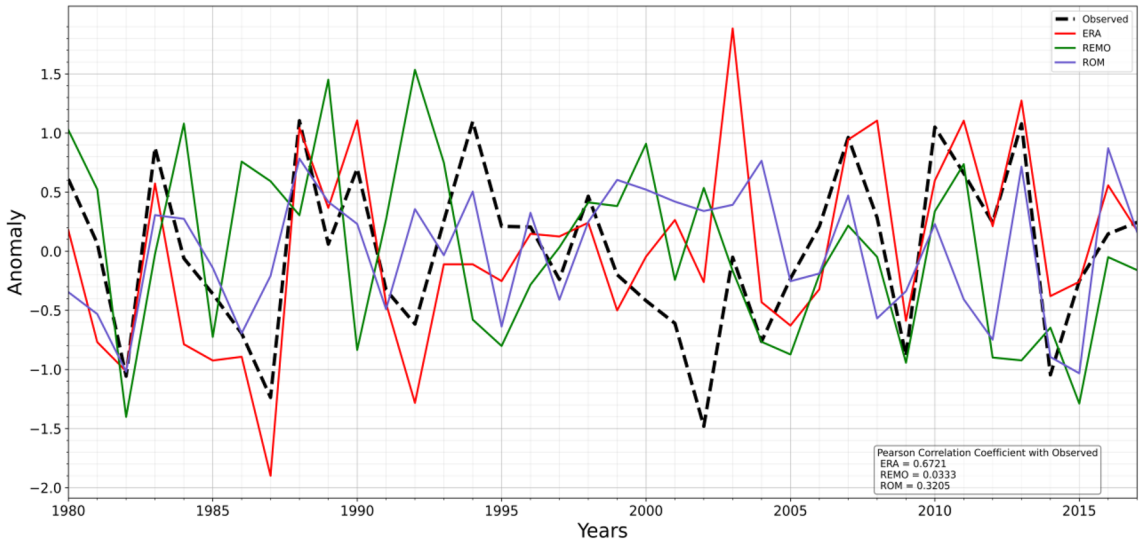

Fig. 5 Interannual Variability of precipitation averaged over Indian land region for ROM, REMO, ERAI, and Observation

the indistinguishable representation of its teleconnections, particularly in the co-occurrence of ENSO and IOD, and partially due to imperfect internal physics.

To further illustrate the performance of ROM's simulation and the added value over its standalone atmospheric component (REMO) in terms of extreme precipitation, we compute the nature of extreme rainfall events using percentile-based precipitation indices (http://etccdi.pacificclimate.org/list_27_indices) for the low precipitation days (R10), moderate wet days (R75), and very wet days (R95) over India (Fig. 6), which have been extensively used as extreme indices (Alexander et al. 2006; Mishra et al. 2020a). Observation shows that the low, moderate, and high precipitation days follow the same pattern with higher values over CI, WG, and IGB and lower values over the southern Peninsular region, NWI, and the northernmost part of India. REMO correctly reproduces the distribution of precipitation of different categories, but it slightly overestimates the extreme precipitation with a slight shift towards South-Central India. This overestimation is substantially reduced in ROM, thus, confirming the advantage of air–sea coupling in reproducing extreme events. Unlike model simulations, the driven forcing (ERAI) shows an underestimation of high extreme precipitation and an overestimation of low precipitation. Interestingly, the distribution of precipitation of different categories in ROM is independent of the distribution in the driven forcing, indicating a greater contribution on the model's internal physics or internal variability rather than parent-driven forcings (external variability) (Sein et al. 2014). The mean precipitation bias in the distribution over India follows the patterns of the high extreme (R95) precipitation with anomalously high R95 values over the south-western CI, a region of large wet bias, suggesting the association of extreme precipitation on JJAS mean precipitation bias.

3.2 Physical mechanisms associated with the bias

The biases in ISMR simulation may be due to different reasons. Thus, it is difficult to find one single factor that explains the ISMR uncertainty. However, to improve the model performance in the future, understanding the possible reasons behind the present biases in the model simulations is crucial for further improvement of the model skill. Thus, an investigation is made in terms of various local and remote drivers and dynamical/thermodynamic processes associated with ISM.

The better represnation of the IO's surface temperature plays a vital role in enhancing the seasonal predictability of ISMR and gets influenced by it (Srivastava et al. 2018). Thus, the realistic representation of SST and its rainfall relationship with ISMR is crucial for the successful simulation of ISMR. Figure 7 shows the seasonal mean SST from ROM and observation (from the HadISST; Rayner et al. 2003) along with corresponding biases.

The figure depicts that the spatiotemporal variability of precipitation is reasonably well-exhibited by ROM. During the pre-monsoon, the spread and intensity of the IO's warm pool significantly control the monsoon onset and sustain moisture supply for the monsoon rainfall. A large region of warm water with SSTs above 29 °C is observed during pre-monsoon over the southeastern Arabian Sea (SEAS). In particular, over the Arabian Sea (AS) mini warm pool region, the SST is found to be ~ 30 °C in observation and earlier studies (Vinayachandran and Shetye 1991). The SST variability over this region is governed by the orographic

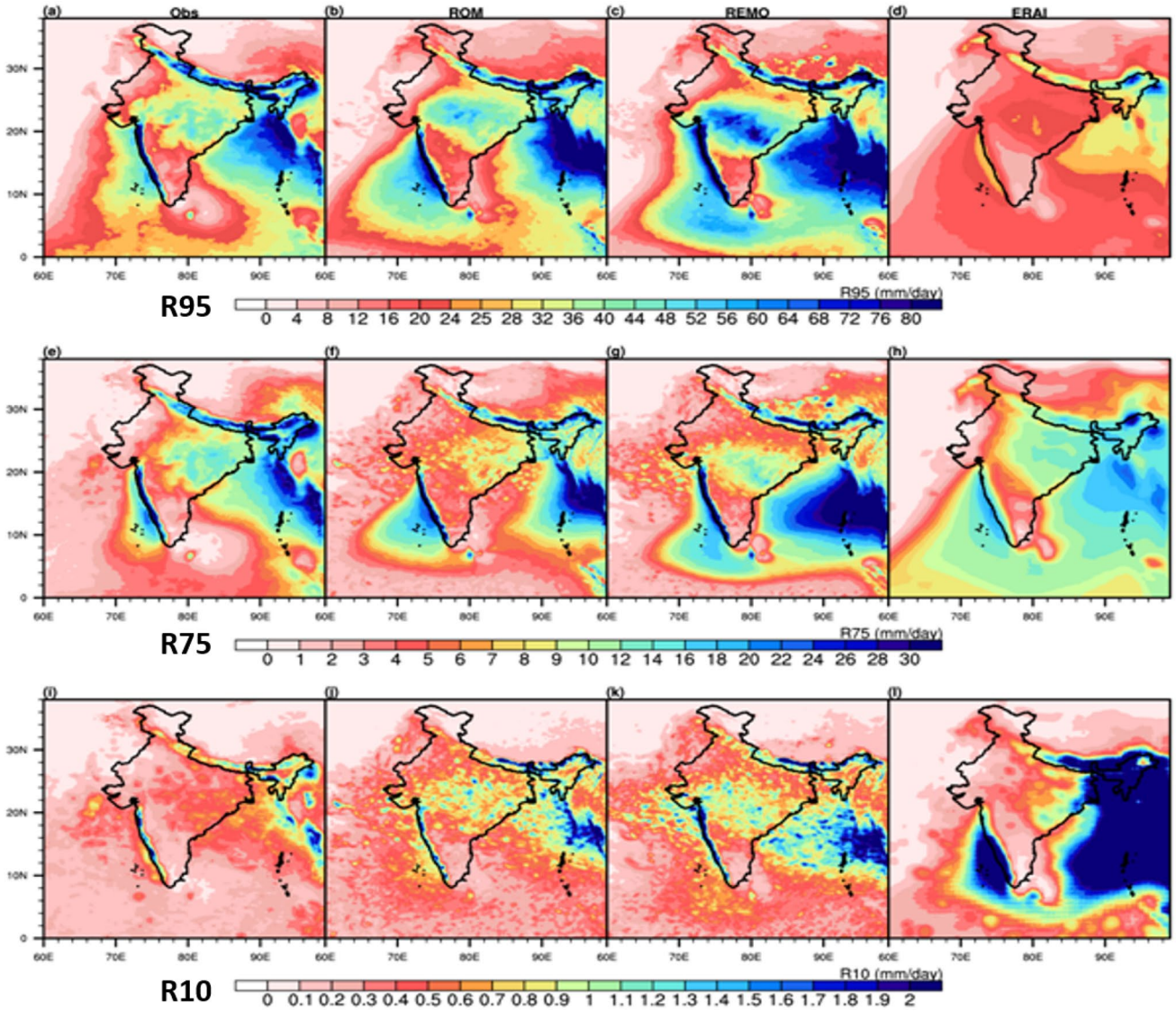

Fig. 6 Percentile-based precipitation indices: R10 for the low precipitation days, R75 for moderate wet days, and R95 for very wet days

effect of the WG and the integrated effect of ocean dynamics and thermodynamics (Vinayachandran and Shetye, 1991). The model capability in correctly simulating the spatial distribution of SST shows the potential for an accurate representation of dynamical and thermodynamical processes. During the summer monsoon season (JJAS), the upwelling of cold waters over the western AS coasts promotes stronger summer monsoon rainfall (Izumo et al. 2008). ROM has a tendency to produce a significant warm bias (1–2 °C) over the AS, particularly over upwelling prone regions along the Somalia coast, due to the reduced upwelling of cold waters associated with the anomalous downwelling Rossby wave and deepening of the thermocline (figure not shown) along with advected warm surface water with equatorial easterlies(Murtugudde et al. 2002; Mishra et al. 2020a). Apart from this, the cold bias (up to 1 °C) over most of the BoB regions is also observed. The cold bias over the BoB can be ascribed to an inadequate representation of the oceanic mixed layer due to the stirring effect of the winds in the absence of coupling wave models (Di Sante et al. 2019; Mishra et al. 2021a), demanding further tuning of the ocean model and coupling wave model towards reducing the warm/cold bias. The relatively warm bias over the western side of the IO basin and the cold bias over the western side of the basin give rise to a positive SST gradient, strengthening the IOD that can contribute to enhanced precipitation, particularly over the eastern AS and western India (Vinayachandarn and Shetye 2009), and hence, the wet bias. During the winter season (December to February; DJF), even though ROM correctly reproduces the regions of warm water over

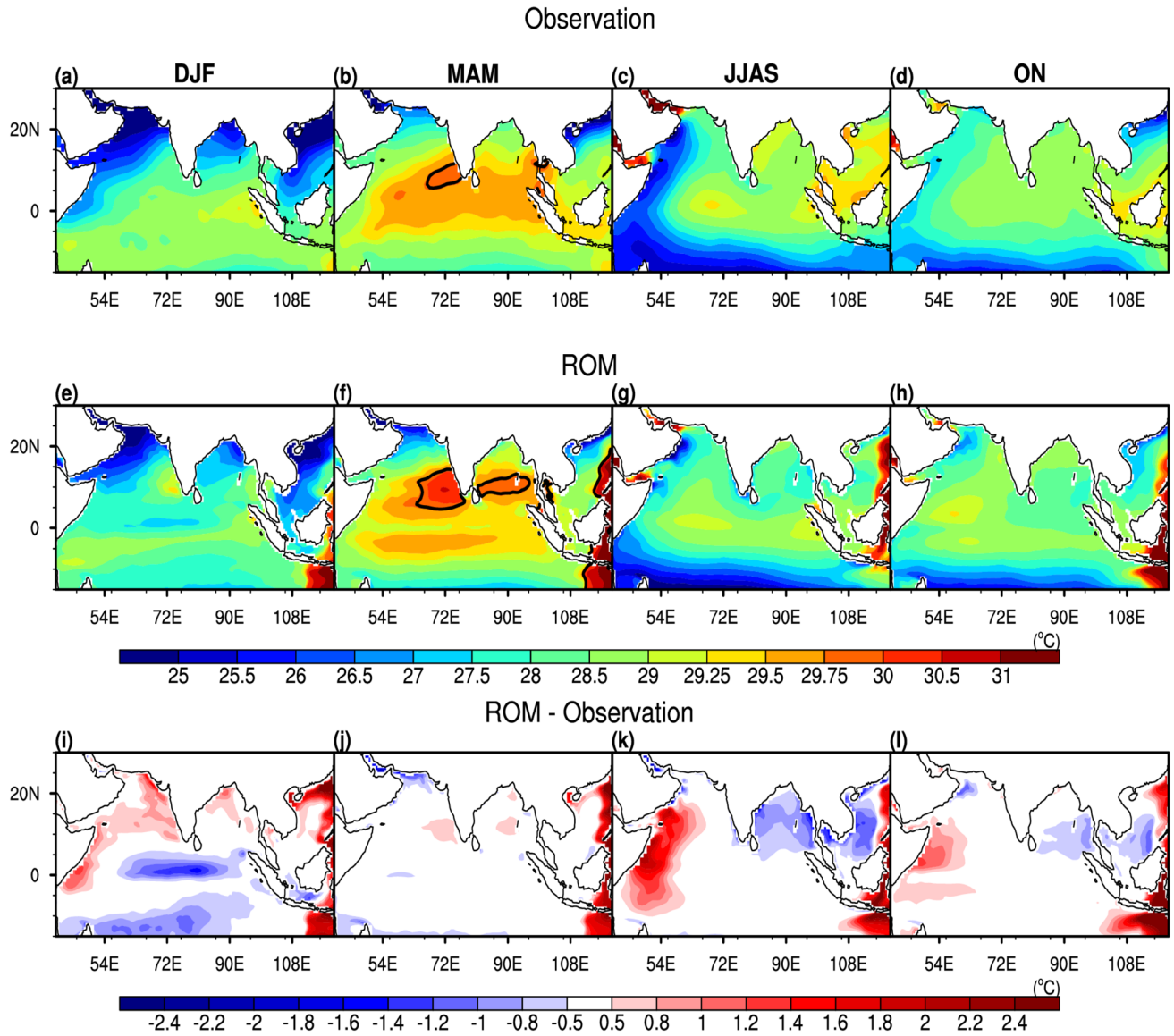

Fig. 7 Seasonal mean sea surface temperature for ROM (a–d), observation (e–h) and bias; ROM-observation (i–l)

southern IO and colder water over AS and BoB, there exists a cold (warm) bias over the regions of warm (cold) water.

Further, we access the model skill in simulating the IOD, one of the key contributors for the IAV of ISMR, biological productivity, and Chlorophyll concentration along the coastal regions of the IO. Dipole mode index (DMI), the difference of area average SST between the western (50°–70° E, 10°–10° N) and the eastern (90°–110° E, 10° S–0°) box on IO (Saji et al. 1999) is used to compute the IOD (Fig. 8). In general, ROM reproduces the positive IOD years (1982, 1994, 1997, 2006, 2015, 2017) and the negative IOD years documented earlier reasonably well. Apart from this, ROM is also able to realistically simulate the temporal evolution of the uneven distribution of IOD events, for example, the increase/decrease of positive IOD (pIOD)/negative IOD (nIOD) in recent decades and past decades. However, ROM produces some unrealistic positive IOD (pIOD) events, particularly in the recent decades, which may be one of the reasons for the positive bias in SST over western AS and wet bias in western India.

The lower level Jets (LLJ) play a very important role in feeding moisture to the Indian land region. The improper representation of the location and strength of these Jets results in uncertainty for the IMSR. Therefore, it is advisable to access these dynamical parameters and their peculiar relationship in ISMR simulation. Thus, we demonstrated the

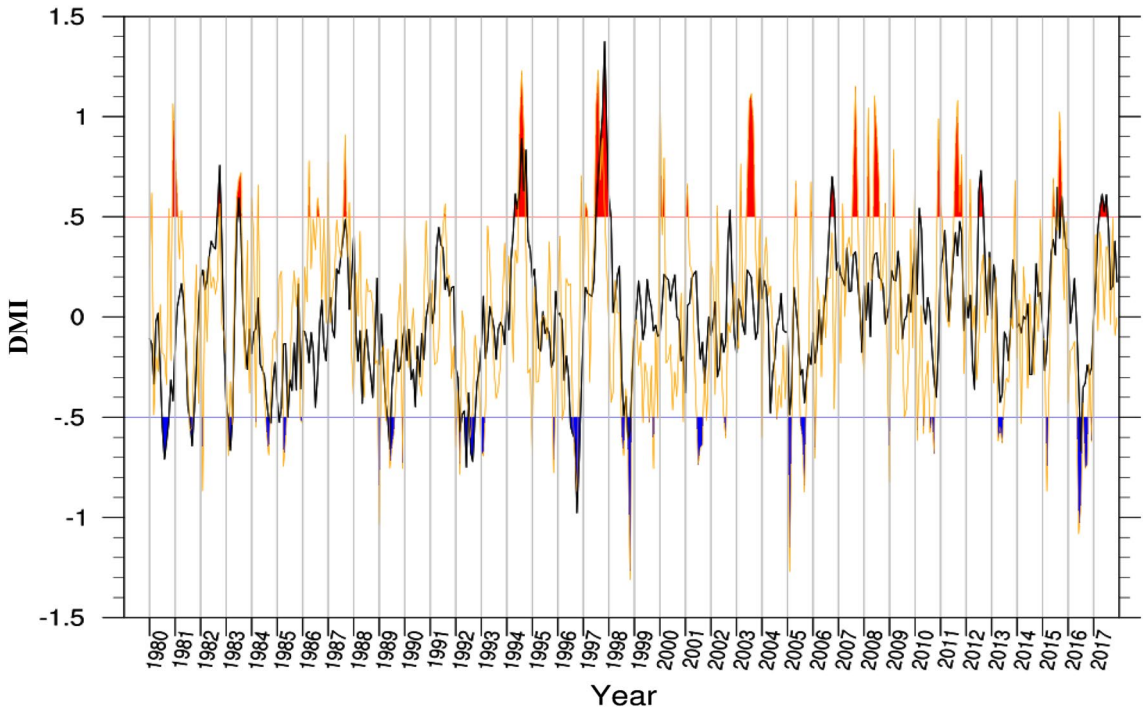

Fig. 8 Monthly Dipole Mode Index for model (orange solid line) and observation (black solid line). The red and blue colors indicate the positive and negative IOD years

model's potential in reproducing vertically integrated JJAS mean moisture flux (VIMF) (Fig. 9).

We observed that both ROM and REMO are able to represent spatial distribution and location of LLJ with a slight discrepancy in magnitude (figure not shown). The maximum VIMF is noticed along the LLJ path and BoB in ERA5. Both models realistically simulate these zones, but REMO has stronger VIMF and LLJ. We computed the bias (model-ERA5) to make the results more robust. REMO shows notable positive bias over eastern AS, southern India, and BoB. The overestimated VIMF over eastern AS in REMO facilitates stronger moisture supply from the AS to Indian continents, favorable conditions for more vigorous monsoon leading to wet bias over western central India. On the contrary, substantial reduction of VIMF and LLJ strength hamper the moisture supply and suppress the precipitation over India, particularly over regions of wet bias, which results in reducing the respective bias. In the REMO, a large bias (overestimation) is noticed over southern India, while precipitation shows a good resemblance to observation over the same region. The divergent flow might advect available moisture from this region to BoB, leading to reduced expected surplus precipitation.

The prevalence and strength of low-pressure systems play a vital role in modulating the ISMR, contributing to 60% of the total rainfall over India and getting influenced by air-sea coupling (Praveen et al. 2015; Levine and Martin 2018; Levine et al. 2020). The long persisting dry bias over the Indian monsoon, especially over the core monsoon region reported in most models (RCMs or GCMs), is not solely attributed to an inaccurate representation of moisture incursion from AS. There is a significant contribution from the BoB LPSs as well. Thus, it is worthwhile to investigate the ROM's potential in simulating the monsoon LPSs. Figure 10 shows LPS during the monsoon season, along with its genesis locations and track for ROM, REMO, and observation. The number of tracks that originated over the ocean is overestimated in REMO and underestimated in ROM compared to ERA5 (Fig. 10a–c). However, in the case of land-originated LPS, REMO and ROM depict an overestimation of similar numbers (Fig. 10d–f). ERA5 tracks have shown a tendency to travel relatively less when compared to the regional models, leading to a number of land LPSs missing out on the filtering restrictions of traveling at least 500kms. Observation indicates lesser LPS genesis frequency over land than over the ocean, with 175 and 224 LPS formed over the land region of CI and the BoB, respectively, during 1980–2017. Most LPSs over BoB bear their genesis over the relatively warmer water of northern BoB and travel northwestward towards CI. Both models simulate this asymmetry of the LPS frequency over

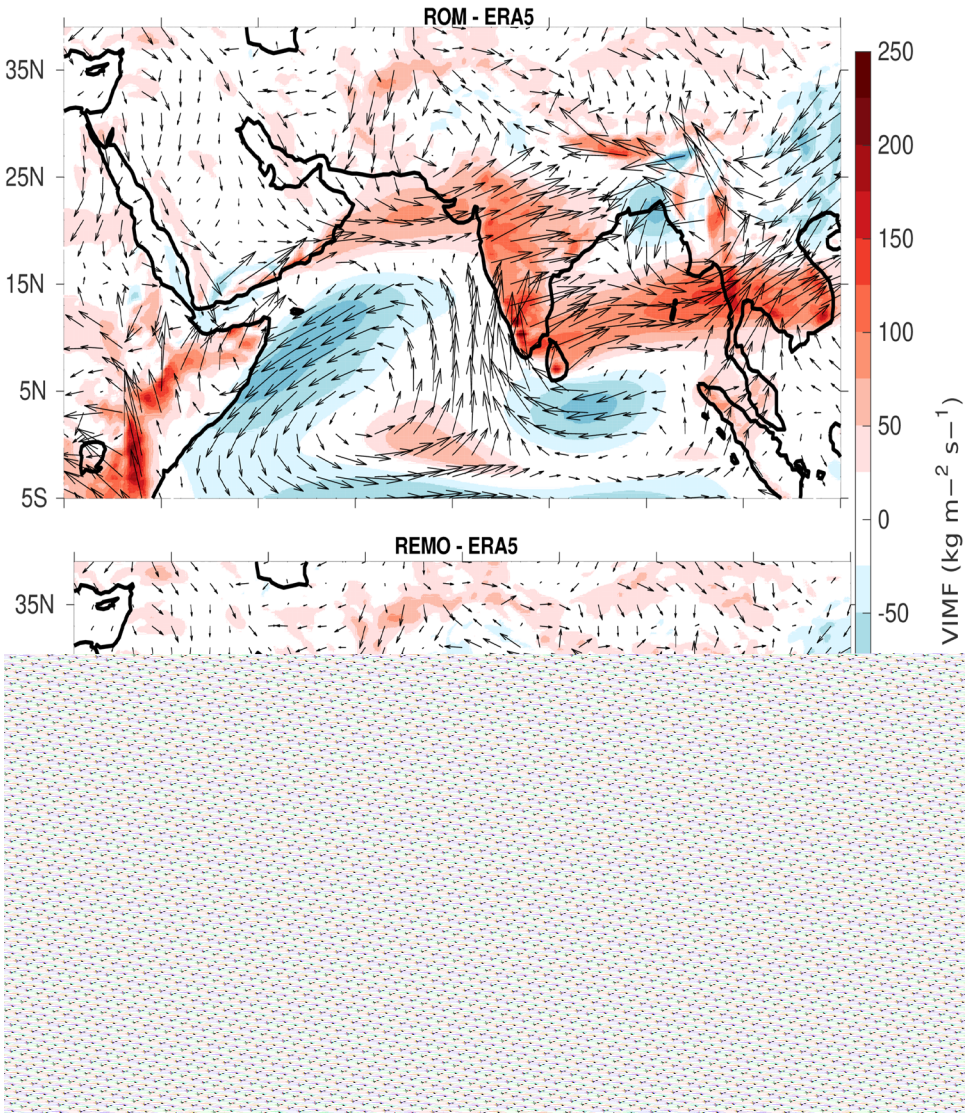

Fig. 9 Vertically integrated JJAS mean moisture flux (VIMF); upper panel; ROM-ERA5 and lower panel; ROM-ERA5

land–ocean and spatial clustering. ROM (REMO) produces 227 (224) and 200 (251) LPSs over land and ocean. Interestingly, the inclusion of air–sea coupling in ROM reduces the LPS frequency due to local negative thermodynamic feedbacks on atmospheric convection that weaken the strength of atmospheric convection by suppressing the atmosphere to ocean net surface heat fluxes and increasing near-surface wind speeds, which cool the SST, reduce latent and sensible heat fluxes and hamper the associated rainfall. This helps in reducing the wet bias over BoB. REMO shows the clustering of LPSs south of 15 N and very few LPS beyond the north of this latitude, whereas ROM shows a good number LPSs north of 20 N over BoB, which is the preferred location of LPS genesis for contributing the landfall over CI (Krishnamurthy and Ajayamohan 2010). Apart from this, an increase of LPS over the land region of CI is also noticed in ROM, compared to REMO, which is consistent with the enhanced precipitation over CI.

Further, an attempt is made to quantify the fraction of total precipitation contributed by LPS over BoB and CI. Figures 11 and 12 depicts the mean precipitation intensity of all the LPS passing through the Impact Box and having their genesis over the ocean(land) for 1980–2017. In general, REMO shows a substantial precipitation bias (overestimation) over WCI, which can be attributed to the tracks traveling for both land and ocean LPS. This can also be observed through Fig. 10, where the lysis cluster over Western India is denser for REMO when compared to ERA5. The low and high regions of LPS related precipitation, particularly the wet bias over Western CI, are co-located with the low and high LPS associated precipitation bias and also with the region of the low and high value of very high extreme precipitation (Fig. 6) and JJAS